Computer Assisted Mechanics and Engineering Sciences, 7: 167–184, 2000.

Implementation of dual grid technique in BEM analysis of 3D contact problems[1]

Sergey Aleynikov and Alexander Sedaev
Dept. of Mathematics, Voronezh State Academy of Architecture and Construction
20-letia Oktyabrya 84, 394006 Voronezh, Russia

(Received March 8, 1999)

The work is devoted to the practical application of dual grids in the boundary element method (BEM). Definitions of dual grids on the plane are given and algorithm constructing dual grid for a given triangulation is described. The problem of utilizing two numerical solutions of one problem defined on the couple of dual grids is considered and the results of this technique are demonstrated. The examples from geomechanics modelling the contact interaction of shallow foundations and elastic bases are presented.

1. Introduction

Application of the boundary element method (BEM) to contact problems [8, 10, 17] and in particular to the problem of interaction of punches and foundations with an elastic half-space of complex structure [2, 5, 18] inevitably leads to dealing with the following general problems:

1. the problem of weak conditionality of corresponding system of algebraic equations;

2. the problem of visualization and interpretation of the numerical solutions obtained;

3. the problem of elimination or reduction of calculating errors.

The paper suggests some practical methods which seem to be useful for the matter. They are based on the notion of grid's duality which is introduced below and is well known in the graph theory [12]. For example, the famous duality of Delaunay triangulation and Dirichlet–Voronoi cells on the plane is the particular case of more general relation between grids which is considered in Sec. 2. We give the detailed definitions of grids' duality and describe the properties of dual grids which are used in the next sections.

In Sec. 3 the algorithm of the Preprocessor generating the dual grid for a given triangulation is presented. The results of its use are given and considered.

Section 4 is devoted to the scheme of applying dual grids in the BEM analysis of spatial contact problems. The accuracy of the suggested method is compared with the other more conventional scheme and the results of our investigations for different contact problems are described.

The last section deals with the utilization of two different numerical solutions of one problem defined in the nodes of a couple of dual grids. We present the algorithm of the postprocessing method which is applied to the results of the BEM analysis of contact problem and to the problem of processing data with random errors.

---

[1]Abbreviated version of this paper was presented at the VII Conference *Numerical Methods in Continuum Mechanics*, Stará Lesná, High Tatras, Slovakia, October 6–9, 1998, and published in its Proceedings.

2. Definitions and properties of dual grids

Long-term application of the BEM for solving the spatial contact problems has shown that besides the initial partition of the contact region, the other partition of the same domain naturally appears. It has a certain structure which is defined (mainly) by the first partition. It turned out that this couple of grids is closely connected with the notion of duality of plane graphs in the graph theory [12]. The Delaunay–Dirichlet duality is a particular example of it [14, 20]. This approach is described in detail below.

Let $\mathbf{A} = \{A_i\}$, $i = 1, 2, \ldots, M$, be a partition of the polygonal domain Q of the plane. We will refer polygons A_i as cells, the vertices of the cells as nodes and the partition $\mathbf{A}$ itself as a grid. If a node P_j is an inner point of Q we will call it an inner node and if it lies on the boundary of Q we will call it a boundary node.

Each grid is also a plane graph G_A which has the same nodes and ribs as the grid $\mathbf{A}$. Adding the polygon A_0 which complements Q to the entire plane we get the partition $\overline{\mathbf{A}}$ of the whole plane. Now we can describe the dual graph G_A^* [12, 20]. Its nodes are any different points $T_0, T_1, \ldots, T_M$ which are corresponded to the cells $A_0, A_1, \ldots, A_M$. Two of such points T_i and T_j are connected by the rib l^* if and only if the corresponding cells A_i and A_j have the common rib l (ribs l and l^* of dual graphs G_A and G_A^* will be referred as *corresponded* ribs). The most clear representation of G_A^* can be obtained if T_i, $i = 1, 2, \ldots, M$, are taken inside corresponding cells A_i, $i = 1, 2, \ldots, M$, and T_0 is the infinite point of the plane.

Each plane graph generates a partition of the plane. So we come to the following

Definition 1. *Two grids* $\mathbf{A}$ *and* $\mathbf{B}$ *on the entire plane are called (mutually) dual if and only if:*

1. *the corresponding graphs* G_A *and* G_B *are dual;*
2. *each node of one grid is contained in the corresponding cell of the other grid;*
3. *each cell of one grid contains only one node of the other grid;*
4. *all ribs of the grids are straight and the corresponded ribs* l *and* l^* *cross each other in the point being inner for both of them.*

The additional conditions 2–4 are necessary for further application of dual grids in numerical analysis.

Now, let Q be a bounded plane domain and $\mathbf{A}$ be a grid on Q. As before we may consider the grid $\overline{\mathbf{A}}$ continuing $\mathbf{A}$ to the entire plane and the dual (in the sense of Definition 1) grid $\overline{\mathbf{B}} = \{\overline{B}_j\}$, $j = 1, 2, \ldots, N$.

Definition 2. *The grid* $\mathbf{B}$*, consisting of polygons* $B_j = \overline{B}_j \cap Q$, $j = 1, 2, \ldots, N$, *where* $\overline{B}_j$ *are the cells of* $\overline{\mathbf{B}}$*, is called 1-type dual to the grid* $\mathbf{A}$ *on the domain* Q.

Figures 1a,b give the examples of dual grids in the sense of Definitions 1 and 2, respectively.

Definition 3. *Two grids* $\mathbf{A}$ *and* $\mathbf{B}$ *on different subdomains* Q_A *and* Q_B *of the plane are called 2-type dual if they can be continued to the dual grids* $\mathbf{A}_1$ *and* $\mathbf{B}_1$ *on the entire plane (Definition 1) and:*

1. *each inner node of one grid is contained in a certain cell of the other grid;*
2. *each cell of one grid contains a unique node (inner or boundary) of the other one.*

It is clear that for a given grid $\mathbf{A}$ there are many different (even in the meaning of the graph theory) dual grids defined on the other domains. Nevertheless all of them are practically identical "near" the set of inner nodes of the grid $\mathbf{A}$ and may be different only in a neighborhood of the boundary of domain Q_A.

Among them the "extremal" dual grids may be selected.

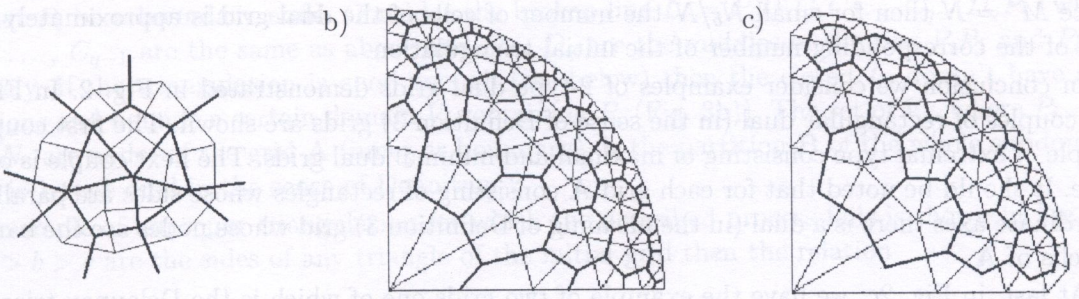

Fig. 1. Couples of dual grids in the sense of Definitions 1, 2, 3, respectively

Definition 4. *The grid* **B** *on domain* Q_B *is called maximal (respectively minimal) for the grid* **A** *on domain* Q_A *if* **A** *and* **B** *are 2-type dual and each node of* **A** *is contained in a certain cell of* **B** *(respectively, each cell of* **B** *contains only an inner node of the grid* **A***).*

The example of such extremal couple of dual grids is demonstrated in Fig. 1c.

It should be noted that in contrast to Definition 1 the grids **A** and **B** introduced by Definition 2 are not mutually dual. The absence of the notion of mutual duality for the grids on a proper subdomain of the plane can not be overcome. In this connection it is interesting to consider the following definitions.

It is easy to see that each grid **A** has a maximal dual grid (for example $\overline{\mathbf{B}}$ from Definition 2) but may not have a minimal dual grid (for example if all nodes of **A** are boundary nodes). Maximal and minimal dual grids are in a certain sense mutually polar.

Proposition 1.

If **B** *is maximal for* **A** *then* **A** *is minimal for* **B**.
If **B** *is minimal for* **A** *then* **A** *is maximal for* **B**.

Since the main aim of the paper is the application of dual grids we omit the proof and turn to the properties of dual grids that may be useful. Mainly we will deal with the 1-type dual grids in the sense of Definition 2.

Let N, L, M and N^*, L^*, M^* be the numbers of nodes, ribs and cells of two dual grids respectively. If $\overline{\mathbf{A}}$ and $\overline{\mathbf{B}}$ are dual grids on the entire plane then, by the definition, $N^* = M$, $L^* = L$, $M^* = N$. For initial grid **A** on a subdomain Q of the plane and the 1-type dual grid **B** $N^* = M + 2N_b$, $L^* = L + 2N_b$ and $M^* = N$, where N_b is the number of boundary nodes of grid **A**. This is because **B** in this case has some new nodes and ribs on the boundary of Q while $\overline{\mathbf{B}}$ has not any. Nevertheless, the number of cells of the 1-type dual grid equals the number of nodes of an initial grid.

In addition, for such dual grids:

1. each inner node of one grid is contained in a certain cell of the other;
2. each cell of an initial grid contains the unique inner node of the dual grid and each cell of the dual grid contains a unique node of an initial grid (inner or boundary);
3. between each two neighbor boundary nodes of an initial grid **A** there is a unique boundary node of the dual grid **B**.

The most typical and important initial grid is a triangulation of Q. Let N_b be the number of boundary nodes of triangulation. Then the well known formula takes place:

$$M = 2(N-1) - N_b\,. \tag{1}$$

Since $M^* = N$ then for small N_b/N the number of cells of the dual grid is approximately equal to half of the corresponding number of the initial triangulation.

In conclusion we consider examples of 2-type dual grids demonstrated in Fig. 2. In Figs. 2a,b, the couples of rectangular dual (in the sense of Definition 3) grids are shown. The first couple is the couple of extremal type consisting of maximal and minimal dual grids. The next couple is of general type. It should be noted that for each grid **A** consisting of rectangles whose sides are parallel to the coordinate axes there is a dual (in the meaning of Definition 3) grid whose nodes are the barycenters of cells of **A**.

At last, in Fig. 2c, we have the example of two grids one of which is the Delaunay triangulation of the convex polygonal subdomain of the plane and the other is the grid of Dirichlet–Voronoi cells on the whole plane. These grids are the classic example of dual graphs in the meaning of the graph theory [14, 20]. It should be noted that they satisfy Definition 1 or Definition 3 if and only if all triangles of the first grid are acute-angled.

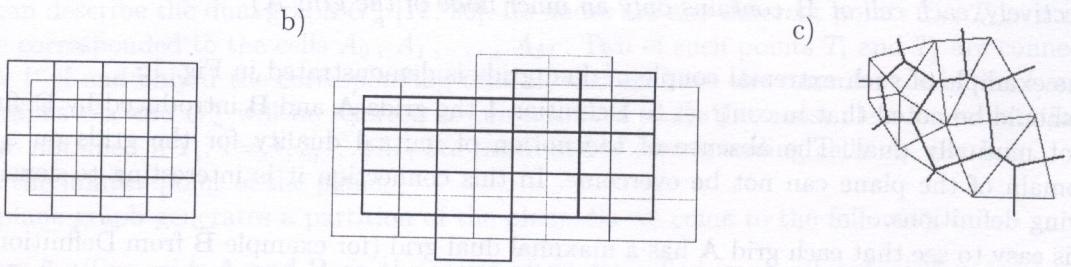

Fig. 2. Couples of dual grids: a), b) rectangular; c) Delaunay–Voronoi duality

3. Case of triangulation and preprocessor

For the most important case when the initial grid **A** is a triangulation of any bounded subdomain Q of the plane we construct and realize an algorithm of the Preprocessor. The main aim of it is to generate 1-type dual grid **B**. The nodes of this grid are taken in the barycenters of triangles of the initial grid and are connected directly if the corresponding triangles have a common side. As a result, each inner node of the initial grid is covered by the cell of the dual grid. The details of the process can be seen in Fig. 3a where $P_{i_1}, P_{i_2}, \ldots, P_{i_q}$ are the neighbor nodes of an inner node P_i and $C_1, C_2, \ldots, C_q$ are the barycenters of the corresponding triangles. Then the broken line $C_1C_2 \ldots C_qC_1$ doesn't have self-intersections and rounds a certain domain V_i that may be taken as the cell of **B** corresponding to P_i.

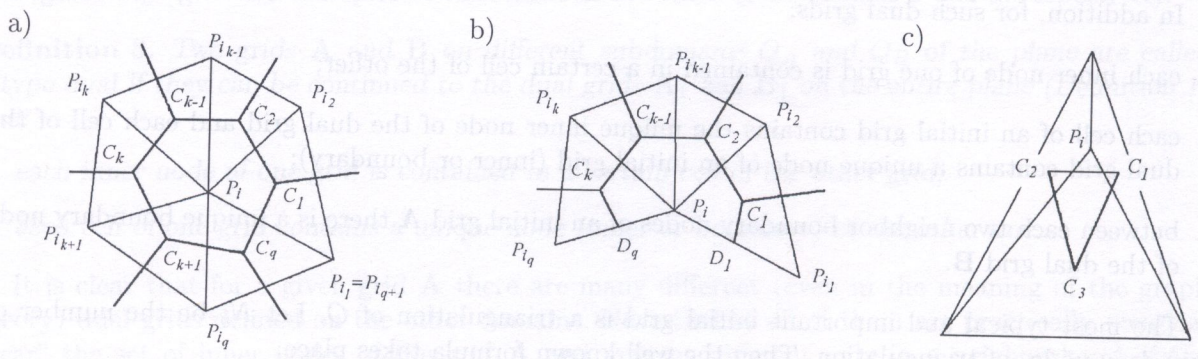

Fig. 3. Construction of dual grid for a given triangulation

Now let P_i be a boundary node. Consider the broken line $L_i = P_i D_1 C_1 C_2 \dots C_{q-1} D_q P_i$, where $C_1, C_2, \dots, C_{q-1}$ are the same as above and D_1, D_q are the middles of the ribs $P_i P_1$ and $P_i P_q$, respectively. If the triangulation is good enough (see below) then the closed L_i doesn't have self-intersections and bounds a certain domain V_i containing P_i (Fig. 3b)). The set of V_i, where P_i, $i = 1, 2, \dots, N$, are nodes of the grid **A** (inner or boundary), is the partition **B** of the whole subdomain Q which is 1-type dual in the sense of Definition 2.

The example of improper triangulation for which the described process fails is shown in Fig. 3c. But if $a > b > c$ are the sides of any triangle of the initial grid then the relation

$$a^2 + b^2 < 5c^2 \tag{2}$$

is a sufficient condition for the described process to lead to the dual grid in the sense of Definition 2. The other sufficient condition of successful preprocessing is the case when each inner node of the triangulation has the coordinates equal the arithmetic mean of the corresponding coordinates of the neighbour nodes and the boundary nodes are situated sufficiently dense along the boundary of Q. In this case we will say that each inner node of the initial triangulation is the arithmetic mean of its neighbour nodes.

The Preprocessor allows us to improve or reconstruct the initial triangulation in order that each inner node be the arithmetic mean of its neighbour nodes or the barycenter of the corresponding cell of the dual grid (see Figs. 4a, b and d, e, respectively.

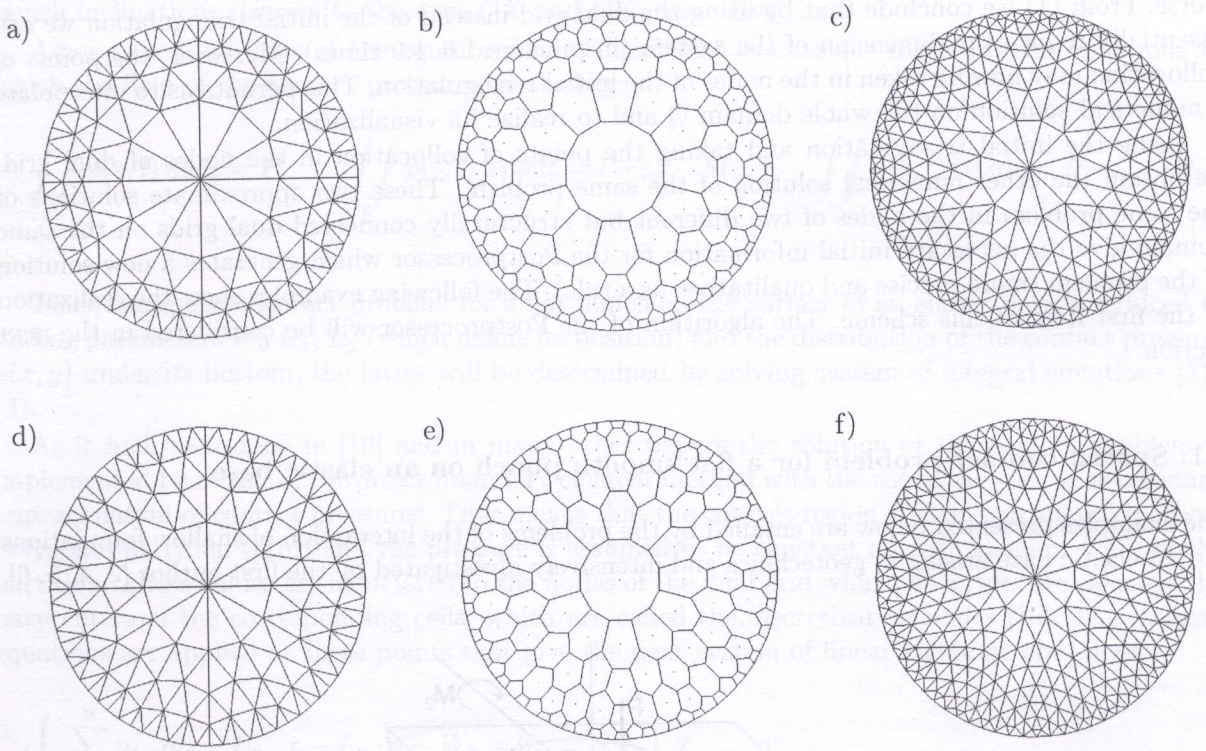

Fig. 4. Grids generated by the Preprocessor

In addition, the Preprocessor generates a new triangulation of the domain Q whose nodes are the nodes of the initial and dual grids taken together, Figs. 4 c,f. This triangulation (which we call general) is necessary for the Postprocessor.

Figures 4, 5 give examples of the Preprocessor's action. The more detailed description of the preprocessor algorithm can be found in [3].

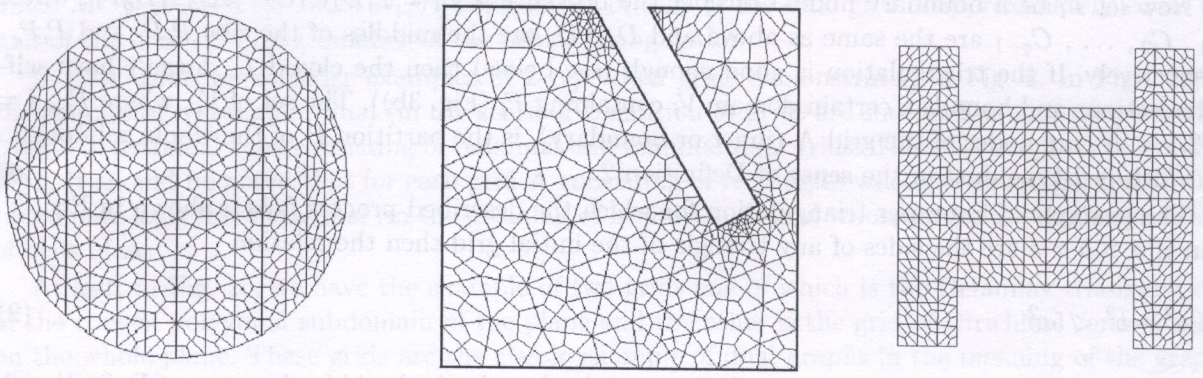

Fig. 5. Results of the Preprocessor application. Dual grids are shown together

4. Application of dual grids in the BEM analysis of spatial contact problems

This section deals with the application of dual grids in the process of solving the spatial contact problems by the boundary element method. The BEM being applied to a problem of mathematical physics leads to a system of algebraic equations. Unfortunately, while the number of elements of a partition increases, the conditionality of the corresponding matrix has a tendency to become worse. From (1) we conclude that by using the dual grid instead of the initial triangulation we can essentially reduce the dimension of the system (in practice 1.6–1.9 times). Moreover, the points of collocation may now be taken in the nodes of the initial triangulation. This permits us to interpolate a numerical solution on the whole domain Q and to realize its visualization.

Using the initial triangulation and taking the points of collocation in the nodes of dual grid, we obtain the other numerical solution of the same problem. These two approximate solutions of the same problem in the nodes of two different but structurally connected dual grids on the same domain give the necessary initial information for the Postprocessor which generates a new solution of the problem (more precise and qualitative, as a rule). The following examples show the realization of the first item of this scheme. The algorithm of the Postprocessor will be considered in the next section.

4.1. Spatial contact problem for a flat smooth punch on an elastic base

The examples presented below are entailed by the problems of the interaction of shallow foundations and an elastic base arising in geotechnics and intensively investigated by the first author [2, 4, 5, 6].

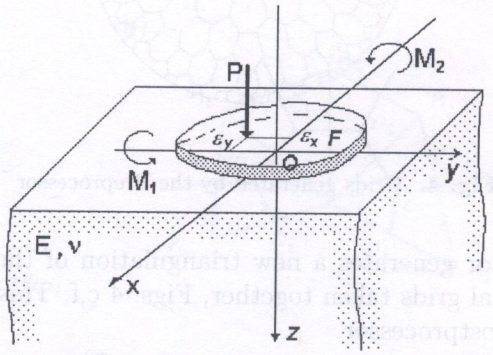

Fig. 6. Flat and smooth punch on an elastic half-space

So, in contrast to [10] where the BEM formulation of the contact problems for elastic bodies is presented, here we deal with the interaction of the flat, smooth and rigid punch that is situated on an elastic half-space $z = 0$ (Fig. 6).

This means that it is sufficient to consider the loading of the punch by the vertical force appled at a point $\mathbf{C}(\varepsilon_x, \varepsilon_y, 0)$ and the couple of moments M_1, M_2 with respect to the coordinate axes. Furthermore, as is customary, we consider that the vertical displacements of the punch and the base surface are equal and the load outside the punch is absent. It is necessary to determine the distribution of the reactive pressures under the punch and the parameters of its displacement as a rigid body. As it had been demonstrated in [14, 13, 16] where the tangential tension had been taken into account, the influence of the friction on the main characteristics of the contact (and the normal pressure especially) is small and we will neglect them in the following consideration.

So, instead of three boundary integral equations [11] we have only one expressing the geometric condition of the punch contact with the half-space

$$\iint\limits_F p(s,t)\,\omega(x,y,s,t)\,\mathrm{d}s\mathrm{d}t = W_0 + L_x \cdot x + L_y \cdot y, \tag{3}$$

where F is the punch contact area with the elastic base; $\omega(x,y,s,t)$ – the corresponding fundamental solution (Green's or influence function) which will be described below; $p(x,y)$ is the function of the contact pressures to be found; W_0 is the vertical displacement of the punch center; L_x, L_y are the punch inclinations relative to the axes OX and OY, respectively.

Among six conditions of the equilibrium it is sufficient to consider three integral equations to which the field of the contact pressures must obey:

$$\iint\limits_F p(s,t)\,\mathrm{d}s\mathrm{d}t = P, \qquad \iint\limits_F p(s,t)\,s\,\mathrm{d}s\mathrm{d}t = P \cdot \varepsilon_x - M_1\,, \qquad \iint\limits_F p(s,t)\,t\,\mathrm{d}s\mathrm{d}t = P \cdot \varepsilon_y + M_2\,. \tag{4}$$

Thus, the spatial contact problem for a flat punch on the surface of an elastic base is reduced to finding parameters W_0 L_x, L_y (which define its position) and the distribution of the contact pressure $p(x,y)$ under its bottom, the latter will be determined by solving system of integral equations (3)–(4).

As it had been done in [10] and in many other papers the solution of the contact problem is implemented by means of the direct boundary element method with the use of the piecewise-constant approximation of contact pressures. That means that the contact region F is approximated by some polygonal partition (grid) and the pressure is assumed to be constant on each element (cell) of the partition. These values are associated to the nodes of the dual grid which, as a rule, are taken in the barycenters of the corresponding cells, which are called the discretization nodes [10]. The integral equations are applied at these points that give the next system of linear algebraic equations

$$\begin{cases} \sum\limits_{j=1}^{n} p_j \cdot d_{ij} - L_x \cdot x - L_y \cdot y - W_0 = 0, \qquad i = 1, 2, \ldots, n; \\ \sum\limits_{j=1}^{n} p_j \cdot \Delta s_j = P; \\ \sum\limits_{j=1}^{n} p_j \cdot x_j \cdot \Delta s_j = P \cdot \varepsilon_x - M_1\,; \\ \sum\limits_{j=1}^{n} p_j \cdot y_j \cdot \Delta s_j = P \cdot \varepsilon_y + M_2\,. \end{cases} \tag{5}$$

Here n is the number of elements (cells) of the partition; p_j is the pressure uniformly distributed on the element j; W_0 is the punch settlement; (x_j, y_j) are the coordinates of the discretization nodes; and

$$d_{ij} = \iint_F \omega(x_i, y_j, s, t)\,\mathrm{d}s\mathrm{d}t.$$

Here, the fundamental solution $\omega(x_i, y_j, s, t)$ is the settlement of a point (s, t) within the domain of the boundary element j due to the unit vertical force applied to the base surface at point (x_i, y_j); Δs_j is the square of the element j.

We use the Bussinesq's fundamental solution for the homogeneous elastic half-space $z = 0$:

$$\omega(x, y, s, t) = \frac{(1-\nu^2)}{\pi E} \cdot \frac{1}{r}, \qquad r = \sqrt{(x-s)^2 + (y-t)^2},$$

and E, ν are the Young's modulus and Poisson's ratio respectively.

At first we compare the exactness of the BEM approximate solutions of the spatial contact problem for the circular punch which is situated on an elastic homogeneous half-space and is loaded by the vertical central force P. This problem has an exact solution [11]

$$W = \frac{P(1-\nu^2)}{2Ea}, \qquad p(r) = \frac{P}{2\pi\sqrt{a^2 - r^2}},$$

where a is the radius of the punch, r is the distance between the center of the punch and a point under it.

For comparison of the BEM approximate solutions we use four grids shown in Fig. 7 and Fig. 4a,b, respectively. The first two grids are polar and contain 400 elements, the third — 216 and the last — 145 elements. The last two grids are dual in the sense of Definition 2.

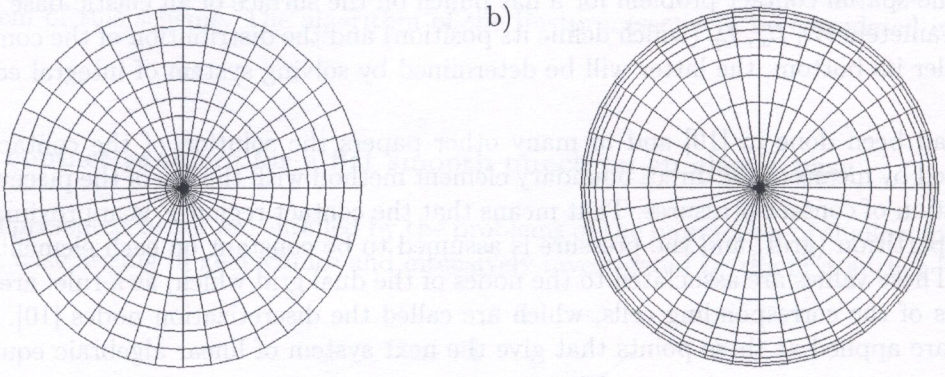

Fig. 7. Polar grids used for solution of contact problem for circular punch

Table 1 and Figure 8 give the results of the BEM applied to the couple of polar grids with and without concentration near the boundary and to the couple of dual grids respectively.

These results show that although the first two grids are more dense, the exactness of the numerical solutions on the dual grids is essentially high especially for the grid of the Dirichlet–Voronoi type that is dual to the initial triangulation and has the least number of elements (cells).

All the results obtained show that the application of the dual grid instead of the initial triangulation does not make the accuracy of the solution worse more than 5–10% and in some cases (as in the previous example) the local and the integral precision may even increase.

Table 1. Properties of approximate solutions of contact problem for circular punch

Type of the grid	Number of elements	Relative square of the contact S/a^2	Relative settling W/a	Degree of conditionality σ	Mean square error
Uniform polar grid	400	3.12869	0.47802	274.0	$4.3265 \cdot 10^{-3}$
Polar grid with the concentration	400	3.12869	0.47114	147.0	$3.3212 \cdot 10^{-2}$
Triangular grid with the concentration	216	3.13761	0.47760	100.6	$1.3489 \cdot 10^{-2}$
Dual grid of Voronoi type	145	3.13761	0.46868	274.2	$1.0686 \cdot 10^{-3}$
Exact solution	—	3.14153	0.46875	—	0

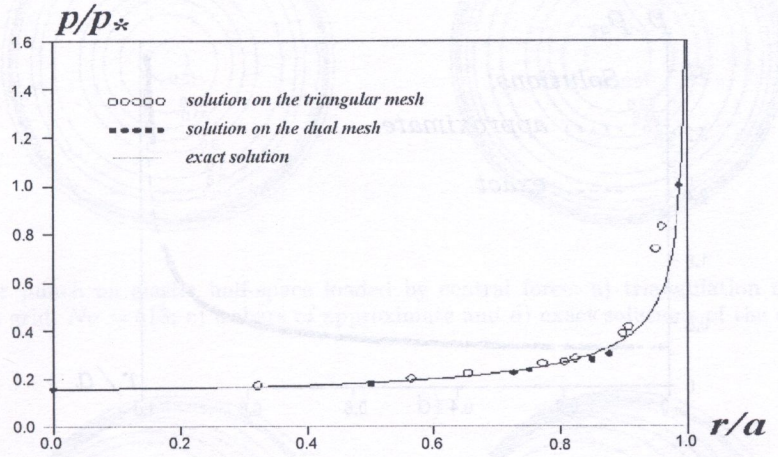

Fig. 8. Exact and approximate contact pressures along the radius of circular punch

4.2. The BEM on non-regular grids and examples of numerical modelling for spatial contact problems

Since the region of the contact for practically important problems has a complicated configuration, the detailed prediction of the contact pressure distribution in the contact domain is very difficult. Theoretically exact solutions are known only for some very restricted and particular classes of such problems where the region of the contact has one of the canonical shapes and the elastic base has a simple structure. On the other hand, the appropriate fundamental solutions of the elasticity theory are known. This approves the application of the boundary element method for numerical modelling of such problems. Our experience shows that this approach may be effective and sufficiently exact but it has some restrictions. The main one is in the necessity to solve the system of algebraic equations of high order with weak degree of coditionality and filled matrix. The other problem is in difficulties connected with visualization and further interpretation of the approximate solution defined on the set of separate points of the domain Q. In both cases the dual grid constructed by the Preprocessor for a given triangulation of Q may be useful. Indeed, according to (1) the dimension of the corresponding algebraic system for dual grid is less than for triangulation (practically more than 1.5 times) and since the points of collocation may be taken in the nodes of the triangulation one can easily extrapolate the numerical solution onto whole domain piecewise linearly (linearly within each triangle).

According to this idea we observe the following sequence of actions.

At first we do the triangulation of the contact domain Q trying to satisfy the following conditions: (a) triangles should be approximately of the same size; (b) their form should be close to equilateral triangle; (c) the inner nodes of the triangulation should be equal to the arithmetic mean of their neighbour nodes.

Next, we turn to the 1-type dual grid (which is constructed by the Preprocessor) and using the BEM find a corresponding approximate solution.

At last we continue the approximate solution from the nodes of the triangulation onto the whole domain Q and fulfill its visualization by means of isobars.

Below we present some examples of this technique. The first of them is the circular rigid punch loaded by a central force. It is the same problem that considered above but in this case we use the non-regular grid close to uniform. Since in contrast to the previous example our grid is non-regular and has no concentration near the boundary, we have to use the dual grid having 513 cells. As a result we obtain an acceptable approximate solution which is demonstrated and compared with the exact solution in Fig. 9 and 10.

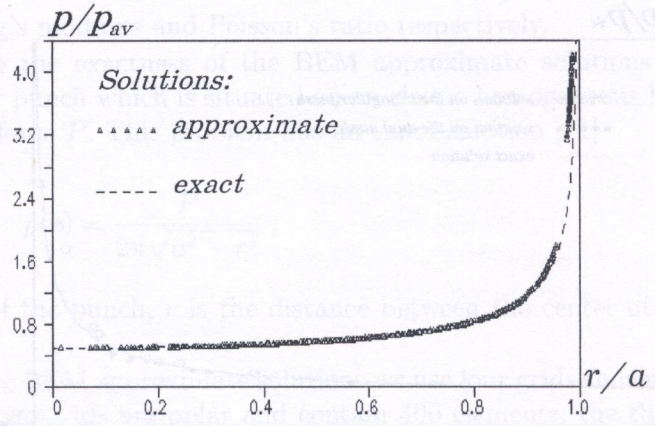

Fig. 9. Exact and approximate contact pressures along the radius of the punch

The corresponding triangulation and dual grids are also presented. The relative settlement of the punch $W/a = 0.47216$ and the number of conditionality $\sigma = 115.3$.

The comparison of this and previous example show that the application of grids with the concentration near the boundary give the considerable gain in the number of grid cells and in dimension of the corresponding system of equations. But the last example shows that non-regular close to uniform initial triangulation is also acceptable.

We also consider the coefficient $K_{TV} = N_T/N_V$, where N_T and N_V are the numbers of the cells of the initial triangulation and the dual grid, respectively. This coefficient shows the reduction of the discrete system connected with the problem. In the example $K_{TV} = 1.84$.

The following example is devoted to the eccentric loading of a circular rigid punch situated on an elastic half-space. In Figs. 11a,b one can see the isobars when the eccentricity of the loading force and consequently the corresponding tipping moment are small. In this case the region of the contact is the entire circle and the corresponding exact solution exists [1]:

$$p(x,y) = \frac{1}{2\pi a^2\sqrt{a^2-r^2}}(P\cdot a + 3\cdot\frac{x}{a}\cdot M), \qquad W(x,y) = W_0 + \delta\cdot\frac{x}{a},$$

where the central loading force P, the tipping moment M around Y-axis, the central displacement W_0 (due to impression) and the maximal displacement δ (due to tipping) are connected as follows

$$P = \frac{2a^2E}{(1-\nu^2)}\cdot\frac{W_0}{a}, \qquad M = \frac{4Ea^3}{3(1-\nu^2)}\cdot\frac{\delta}{a}.$$

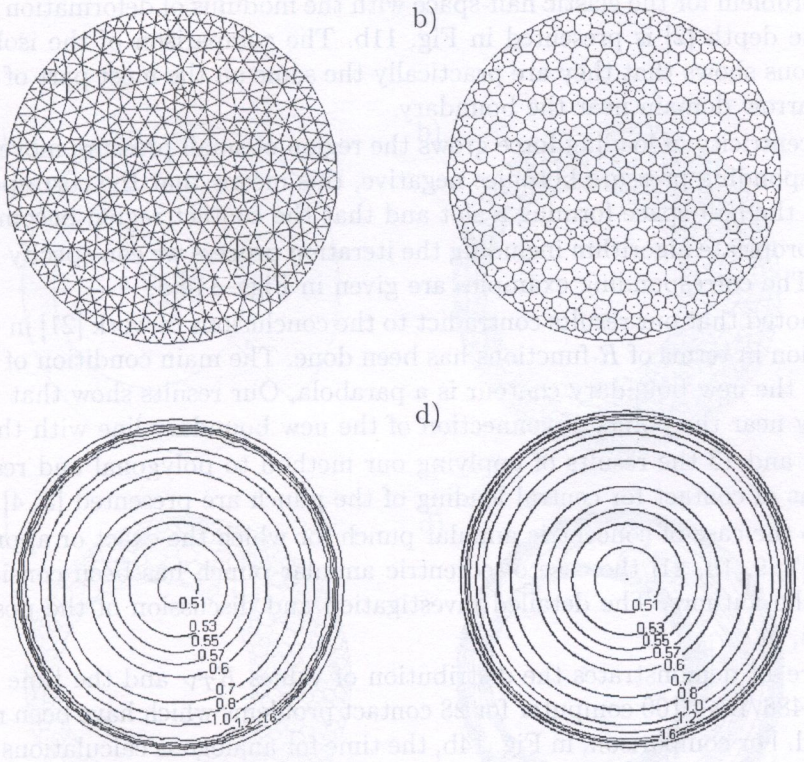

Fig. 10. Circular punch on elastic half-space loaded by central force: a) triangulation of contact region, $N_T = 944$; b) dual grid, $N_V = 513$; c) isobars of approximate and d) exact solutions of the contact problem

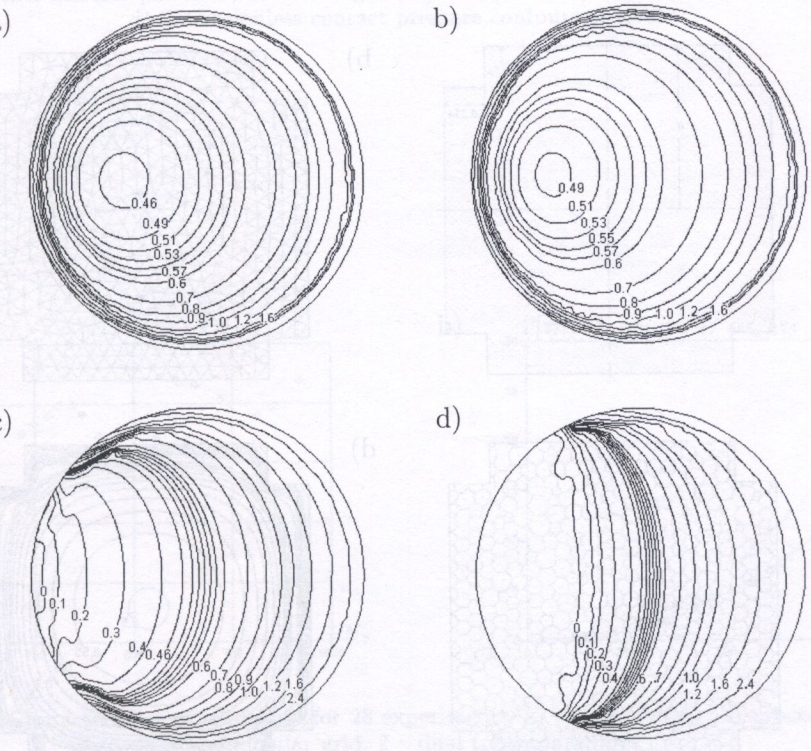

Fig. 11. Contours of levels of dimensionless contact pressure for circular punch loaded by eccentric force ($N_V = 513$): a), c), d) deformation modulus $E = E_0 = \text{const.}$; b) $E = E_0(1 + z/h)$, $h/a = 1$; a), b) $\varepsilon_x = 0.15a$; c) $\varepsilon_x = 0.35a$; d) $\varepsilon_x = 0.5a$

The analogous problem for the elastic half-space with the modulus of deformation $E = E_0(1+Bz/h)$ growing with the depth [2] is presented in Fig. 11b. The comparison of the isobars for exact and numerical solutions shows that they are practically the same on the most part of the contact region excluding the narrow domain near the boundary.

While the eccentricity of loading force grows the region of small pressure moves to the boundary. When the corresponding pressure becomes negative, this means that the corresponding part of the punch rises over the half-space forming a slot and that the contact region becomes smaller.

Using the appropriate algorithm including the iteration process we can specify the shape of a new contact region. The corresponding examples are given in Figs. 11c,d.

It should be noted that our results contradict to the conclusions of work [21] in which the attempt to give the solution in terms of R-functions has been done. The main condition of that work was the assumption that the new boundary contour is a parabola. Our results show that this assumption is wrong, especially near the points of connection of the new boundary line with the circle.

In Figures 12 and 13 the results of applying our method to polygonal and respectively doubly-connected regions of contact for central loading of the punch are presented [3, 4].

In contrast to the case of concentric annular punch for which the exact or approximate solutions are well known [7, 9, 19, 21] the case of eccentric annular punch has been considered for the first time by one of the authors. The detailed investigation and discussion of the possible applications are given in [4, 5, 6].

At last, Figure 14 demonstrates the distribution of values K_{TV} and the time of calculations by the IBM PC AT 486/DX4 100 computer for 28 contact problems which have been numerically solved using our method. For comparison, in Fig. 14b, the time for analogous calculations for corresponding triangulations are presented.

As conclusion it should be noted that at least for the case of contact problems the described method gives a universal and acceptable approach overcoming the difficulties mentioned in the beginning of the section.

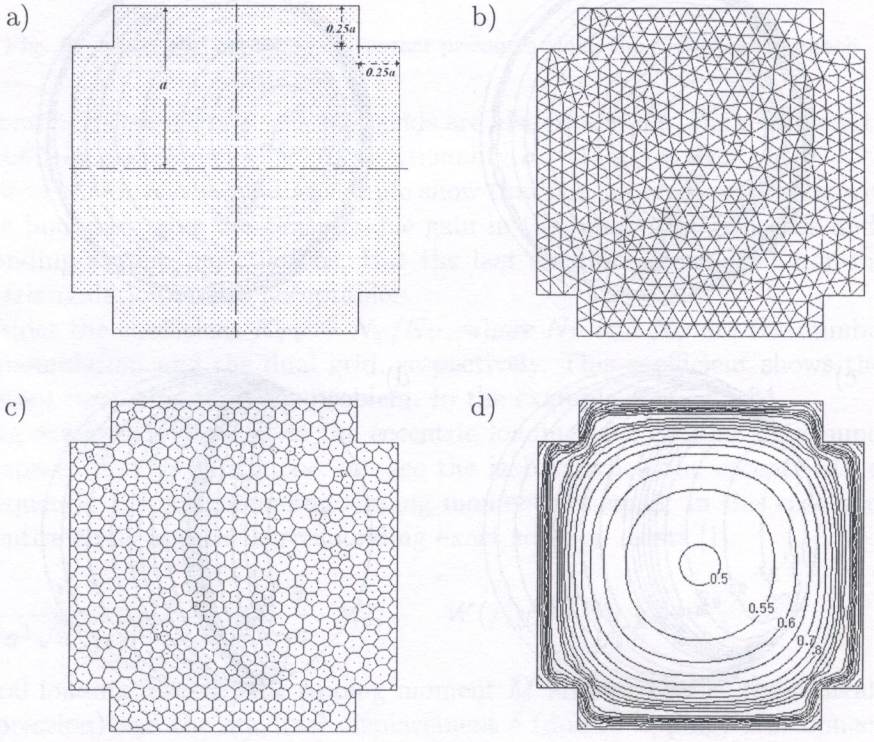

Fig. 12. Square punch with corner excisions loaded by central force: a) contact region; b) triangulation, $N_T = 1118$; c) dual grid, $N_V = 608$; d) dimensionless contact pressure contours of levels

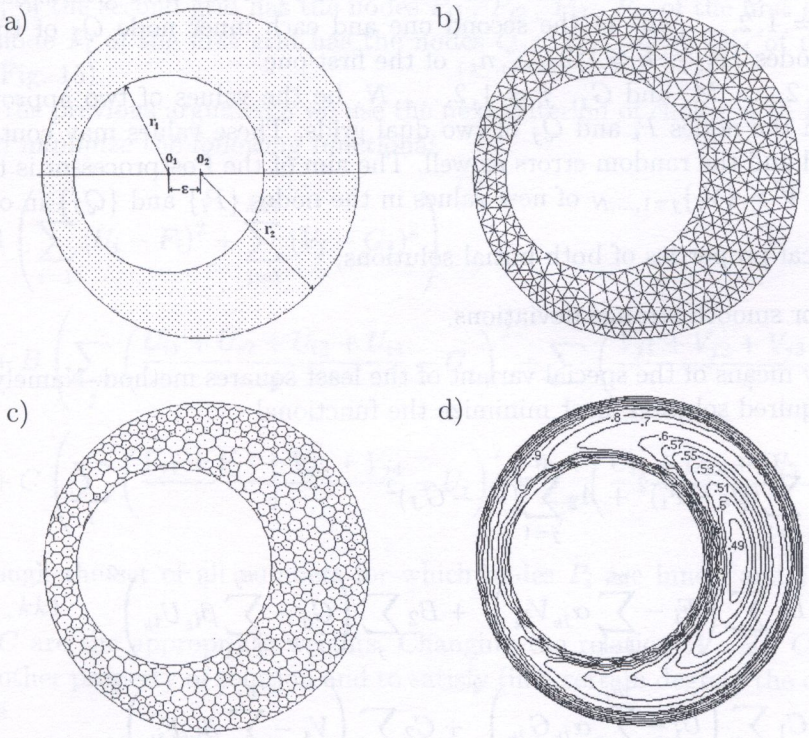

Fig. 13. Eccentric annular punch: a) contact region; b) triangulation, $N_T = 929$; c) dual grid, $N_V = 539$; d) dimensionless contact pressure contours of levels

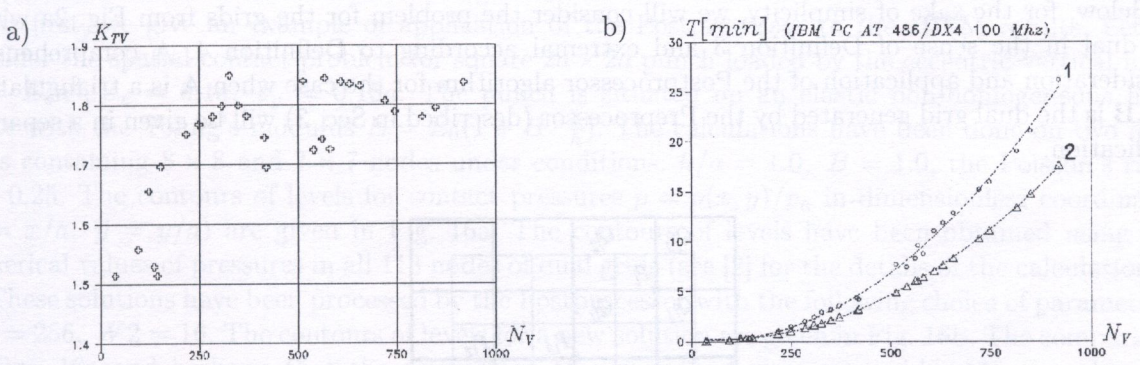

Fig. 14. Characteristics of effectivity for 28 experiments: a) values of K_{TV}; b) processor time: 1 – triangular grid, 2 – dual (polygonal) grid

5. Postprocessor algorithm and its applications

Now we describe the idea of the Postprocessor that uses the couple of numerical solutions being defined on two dual grids. As we know each inner node P_i of the first grid is surrounded by the nodes $\{Q_{j_k}\}$, $k = 1, 2, \ldots, m_i$, of the second one and each inner node Q_j of the second grid is rounded by the nodes $\{P_{i_k}\}$, $k = 1, 2, \ldots, n_i$, of the first one.

Let F_i, $i = 1, 2, \ldots, M$, and G_j, $j = 1, 2, \ldots, N$, be the values of two approximate solutions of one problem in the nodes P_i and Q_j of two dual grids. These values may contain errors of the numerical method and the random errors as well. The aim of the Postprocessor is to derive the sets $\overline{U} = \{U_i\}_{i=1,\ldots,M}$, $\overline{V} = \{V_j\}_{j=1,\ldots,N}$ of new values in the nodes $\{P_i\}$ and $\{Qj\}$ in order to:

(a) preserve typical properties of both initial solutions;

(b) to eliminate or smooth strange deviations.

This is done by means of the special variant of the least squares method. Namely, the sets $\overline{U}$ and $\overline{V}$ forming the required solution must minimize the functional

$$
\begin{aligned}
H(\overline{U},\overline{V}) = {} & A_1 \sum_{i=1}^{M} (U_i - F_i)^2 + A_2 \sum_{j=1}^{N} (V_j - G_J)^2 \\
& + B_1 \sum_i \left(F_i - \sum_{k=1}^{m_i} \alpha_{j_k} V_{j_k} \right)^2 + B_2 \sum_j \left(G_j - \sum_{k=1}^{n_j} \beta_{i_k} U_{i_k} \right)^2 \\
& + C_1 \sum_i \left(U_i - \sum_{k=1}^{m_i} \alpha_{j_k} G_{j_k} \right)^2 + C_2 \sum_j \left(V_j - \sum_{k=1}^{n_j} \beta_{i_k} F_{i_k} \right)^2 \\
& + D_1 \sum_i \left(U_i - \sum_{k=1}^{m_i} \alpha_{j_k} V_{j_k} \right)^2 + D_2 \sum_j \left(V_j - \sum_{k=1}^{n_j} \beta_{i_k} U_{i_k} \right)^2 .
\end{aligned}
$$

Here the sums without limits are taken for all inner nodes and $\sum_{k=1}^{m_i} \alpha_{j_k} = \sum_{k=1}^{n_j} \beta_{i_k} = 1$. The positive coefficients α_{j_k} and β_{i_k} are defined by the mutual disposition of the nodes P_i and Q_j. The numbers A_1, A_2, B_1, B_2, C_1, C_2, D_1, D_2, are weights that may be selected in order to accent one or another property of the new solution and should be chosen in connection with the specific character of the problem considered.

Below, for the sake of simplicity, we will consider the problem for the grids from Fig. 2a which are dual in the sense of Definition 3 and extremal according to Definition 4. A comprehensive consideration and application of the Postprocessor algorithm for the case when **A** is a triangulation and **B** is the dual grid generated by the Preprocessor (described in Sec. 3) will be given in a separate publication.

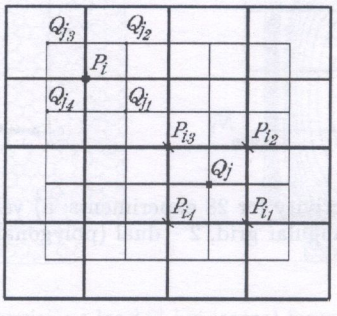

Fig. 15. The neighbour nodes for couple of dual rectangular grids

Let A be a rectangular homogeneous grid containing $kk = k \cdot k$ nodes and B be the rectangular grid containing $kk1 = (k-1) \cdot (k-1)$ nodes which are the barycenters of corresponding elements of the first grid.

Each node Q_j of the second grid has the nodes P_{i1}, P_{i2}, P_{i3}, P_{i4} of the first grid as neighbours and each inner node P_i of the first grid has the nodes Q_{j1}, Q_{j2}, Q_{j3}, Q_{j4} of the second grid as neighbours (see Fig. 15).

According to the previous arguments we use the next criterion of choice of U_i and V_j: *the values U_i and V_j should minimize the following functional*

$$H(\overline{U},\overline{V}) = A\left(\sum_{i=1}^{kk}(U_i - F_i)^2 + \sum_{j=1}^{kk1}(V_j - G_j)^2\right)$$
$$+ B\left(\sum_j\left(\frac{U_{i1}+U_{i2}+U_{i3}+U_{i4}}{4} - G_j\right)^2 + \sum_i\left(\frac{V_{j1}+V_{j2}+V_{j3}+V_{j4}}{4} - F_i\right)^2\right)$$
$$+ C\left(\sum_i\left(\frac{V_{j1}+V_{j2}+V_{j3}+V_{j4}}{4} - U_i\right)^2 + \sum_j\left(\frac{U_{i1}+U_{i2}+U_{i3}+U_{i4}}{4} - V_j\right)^2\right).$$

Here i runs through the set of all numbers for which nodes P_i are inner, and j runs through all numbers $1, 2, \ldots, kk1$.

Here A, B, C are the appropriate weights. Changing the relation $A : B : C$, it is possible to accent one or another property of solution and to satisfy (in a certain degree) the conditions (a), (b) mentioned above.

The unique extreme point of the functional exists and can be found by solving the corresponding system of linear equations. Its matrix is symmetric and sparse. Some results of applying this method are given below.

5.1. Calculation examples and discussions

Since the Postprocessing method depends on the ratio $A : B : C$ then, without lost of generality, we assume that $B = 16$ is fixed, but $A = W1$ and $C = W2$ are varied to obtain the best result of the method. Here $W1$ is "the weight of the old values" and $W2$ is "the weight of the new values" in the process of choice of new values in the grid nodes.

At first, we give an example of application of the Postprocessor to the BEM results. Let us consider the spatial contact problem for square $2a \times 2a$ punch loaded by the eccentric vertical force $P = E_0 a^2$, $\varepsilon_x = 0.1a$, $\varepsilon_y = 0.15a$. The punch is situated on an elastic non-homogeneous half-space with the Young's modulus $E = E_0(1 + B \cdot \frac{z}{h})$. The calculations have been done on two dual grids containing 8×8 and 7×7 nodes under conditions: $h/a = 1.0$, $B = 1.0$, the Poisson's ratio $\nu = 0.25$. The contours of levels for contact pressures $p = p(x,y)/p_a$ in dimensionless coordinates ($\overline{x} = x/a$, $\overline{y} = y/a$) are given in Fig. 16a. The contours of levels have been obtained using the numerical values of pressures in all 113 nodes of dual grids (see [2] for the details of the calculations).

These solutions have been processed by the Postprocessor with the following choice of parameters: $W1 = 256$, $W2 = 16$. The contours of levels for a new solution are given in Fig. 16b. The comparison of Figs. 16a and b shows that the application of our method gives a considerable smoothing of numerical results. Unfortunately, the exact solutions for this class of spatial contact problems are unknown (as a rule). So we have no opportunity to compare the accuracy of numerical solutions before and after postprocessing.

Now we describe the application of the Postprocessor to the results of experiments with random errors. To demonstrate the method potentialities the following model is used. Let a function of two variables be defined on the square and let a couple of 2-type dual rectangular grids of this

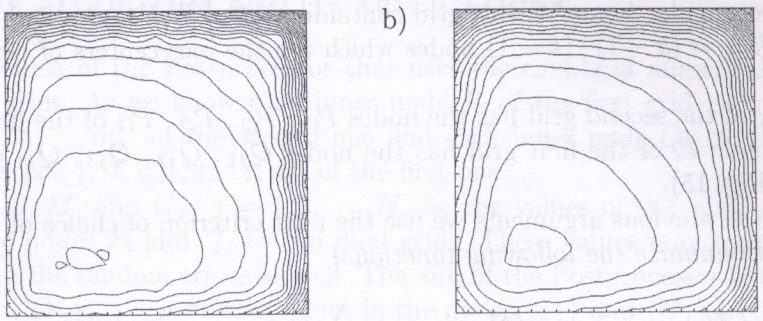

Fig. 16. Isobars; a) before and b) after post-processing

square be given. We define the values of this function in the nodes of the grids by $\mathbf{f} = \{f_i\}_{i=1}^{kk}$ and $\mathbf{g} = \{g_j\}_{j=1}^{kk1}$, respectively. Let the upper bound q of random errors be known. Then using the random numbers $\{r_k\}$, uniformly distributed on the interval $[-q, q]$, we obtain the new values $\overline{f}_i = f_i + r_{k_0+i}$, $i = 1, 2, \ldots, kk$, and $\overline{g}_j = g_j + r_{k_1+j}$, $j = 1, 2, \ldots, kk1$, which contain the random errors. The general deviations are estimated by the quantities

$$df_{\text{old}} = \frac{1}{kk}\left(\sum_{1}^{kk}(\overline{f}_i - f_i)^2\right)^{\frac{1}{2}}, \qquad dg_{\text{old}} = \frac{1}{kk1}\left(\sum_{1}^{kk}(\overline{g}_i - g_i)^2\right)^{\frac{1}{2}}.$$

Then, applying the Postprocessor to $\{\overline{f}_i\}$ and $\{\overline{g}_j\}$, we obtain the new values $\{f'_i\}$ and $\{g'_j\}$ in the nodes of the first and the second grids, respectively. The new general deviations from the exact values are estimated as follows

$$df_{\text{new}} = \frac{1}{kk}\left(\sum_{1}^{kk}(f'_i - f_i)^2\right)^{\frac{1}{2}}, \qquad dg_{\text{new}} = \frac{1}{kk1}\left(\sum_{1}^{kk}(g'_i - g_i)^2\right)^{\frac{1}{2}}.$$

Comparison of new and old estimates gives the objective information about the method.

Such experiments have been made for unit square $[0,1] \times [0,1]$ and three functions $f_1 = (x - 0.5)(y - 0.5)$, $f_2 = x^2 + y^2$ and $f_3 = \sin \pi x \cos \pi y$. In all cases the first grid contains 11×11 nodes and the second one — 10×10 nodes. The results of the experiments are presented in Table 2 and Figs. 17–19.

In Figs. 17, 18, 19 the corresponding contours of levels are given. In case a), the contours of levels for the initial function are demonstrated. In case b) — the contours of levels with random errors are shown and in case c) — the contours of levels after the application of the Postprocessor are presented.

These results show that the method can increase the accuracy in 2–4 times. Its efficiency depends on the function. The function f_1 has the property: the value in the inner node equals the arithmetic mean of the values in the neighbour nodes. So we obtain the best result for the big ratio $W2/W1$. The other functions do not satisfy this property. The best result for f_2 takes place when the ratio $W2/W1 = 1$ and for f_3 — when $W2/W1$ is small. The experiments show that if the number of grid nodes (density of the grid) increases then the accuracy of the method also increases.

Our experience shows that the correct application of the Postprocessor is a strong and useful tool.

Table 2. Application of the Postprocessor to the data with random errors

Function	q	$W1$	$W2$	df_{old}	dg_{old}	df_{new}	dg_{new}
$f_1 = (x - 0.5)(y - 0.5)$	0.06	16	256	0.0255	0.0323	0.0117	0.0089
$f_2 = x^2 + y^2$	0.03	64	64	0.0127	0.0173	0.0041	0.0036
$f_3 = \sin \pi x \cos \pi y$	0.06	64	16	0.0255	0.0323	0.0145	0.0151

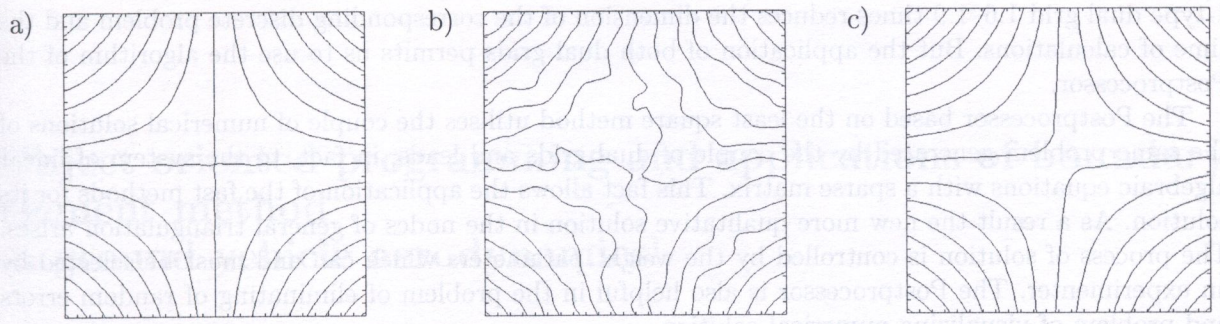

Fig. 17

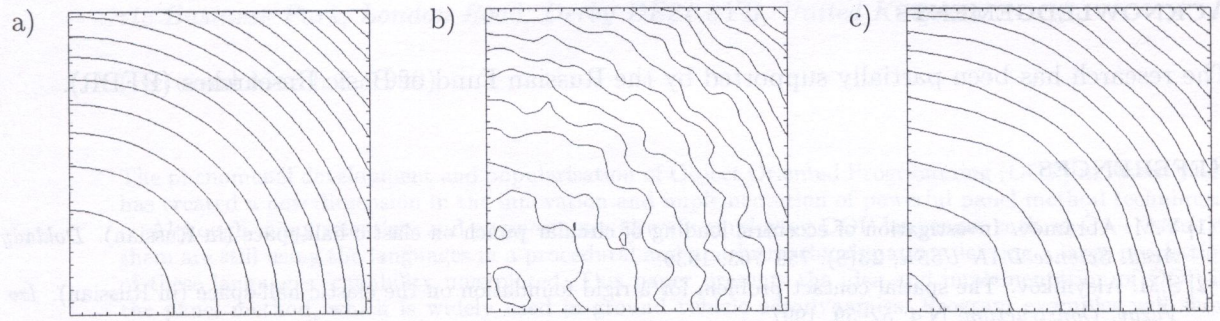

Fig. 18

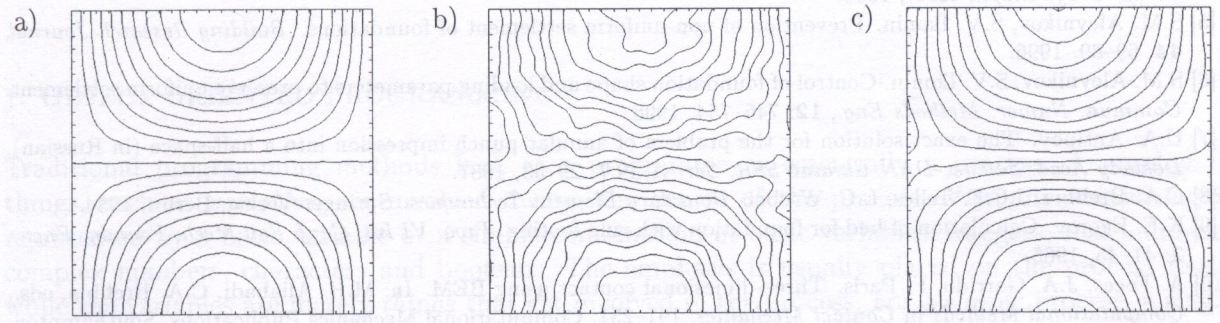

Fig. 19

6. Conclusions

The aim of the paper is to attract attention to possibilities of a new technique based on the notion of grids duality. It has been shown that the application of dual grids is useful and effective at all stages of solving the spatial contact problems using the BEM: a) at the stage of partition; b) at the stage of numerical calculation of solutions and c) at the stage of their analysis and postprocessing.

At the stage of partition this approach (on the base of a given triangulation) allows us to obtain the new partition of the same domain onto the cells of Dirichlet–Voronoi type. The number of elements of this partition 1.6–1.9 times low than the corresponding number for the initial triangulation. Moreover, the application of our technique makes it possible to rebuild both grids, to rise their quality and to obtain a new dense and qualitative *general triangulation* of the same domain. In addition the corresponding algorithm is fast and is not memory expensive.

At the stage of approximate solution of the spatial contact problem by means of the BEM one has an opportunity to select the desirable partition from those mentioned above. The use of

1-type dual grid 1.6–1.9 times reduces the dimension of the corresponding discrete problem and the time of calculations. But the application of both dual grids permits us to use the algorithm of the Postprocessor.

The Postprocessor based on the least square method utilises the couple of numerical solutions of the same problem generated by the couple of dual grids and leads, in fact, to the system of linear algebraic equations with a sparse matrix. This fact allows the application of the fast methods for its solution. As a result the new more qualitative solution in the nodes of general triangulation arises. The process of solution is controlled by the weight parameters which can and must be selected by an experimenter. The Postprocessor is also helpful in the problem of eliminating of random errors and problem of visualizing numerical solution.

The properties mentioned above have been practically verified in a great number of experiments.

Acknowledgements

The research has been partially supported by the Russian Fund of Basic Researches (RFBR).

References

[1] V.M. Abramov. Investigation of eccentric loading of circular punch on elastic half-space (in Russian). *Doklady Acad. Science-DAN USSR*, **23**(8): 759–763, 1939.

[2] S.M. Aleynikov. The spatial contact problem for a rigid foundation on the elastic half-space (in Russian). *Izv. Vuzov. Construction*, **N 4**: 52–59, 1997.

[3] S.M. Aleinikov, A.A. Sedaev. Dual grids and their application in the Boundary Element Method. *Computational Mathematics and Mathematical Physics*, **38**: 228–241, 1999.

[4] S.M. Aleynikov, S.V. Ikonin. Patent of Russian Federation N 2043462 *"Foundation for buildings of tower type on the wedge-shaped base"*, 1995.

[5] S.M. Aleynikov, S.V. Ikonin. Prevention of non-uniform settlement of foundations. *Building Research Journal*, **44**: 69–89, 1996.

[6] S.M. Aleynikov, S.V. Ikonin. Control of foundation shape and loading parameters to preserve uniform settlement. *Commun. Numer. Methods Eng.*, **12**: 745–754, 1996.

[7] U.A. Antipov. The exact solution for the problem of annular punch impression into a half-space (in Russian). *Doklady Acad. Science-DAN Ukraine SSR, Ser. A*, **N 7**: 29–33, 1987.

[8] C.A. Brebbia, J.C.F. Telles, L.C. Wrobel. *Boundary Element Techniques.* Springer-Verlag, Berlin, 1984.

[9] K.E. Egorov. Calculation of bed for foundation with ring footing. *Proc. VI Int. Conf. Soil Mech. Foundn. Engn.*, **2**: 41–45, 1965.

[10] A. Foces, J.A. Garrido, F. Paris. Three-dimesional contact using BEM. In: M.H. Aliabadi, C.A. Brebbia, eds., *Computational Methods in Contact Mechanics*, 191–231. Computational Mechanics Publications, Southampton, 1993.

[11] L.A. Galin. *Contact Problems in the Theory of Elasticity.* Translated by H. Moss. North Carolina State College, Depart. of Math., USA, 1961.

[12] F. Harary. *Graph Theory (in Russian).* Mir, Moscow, 1973.

[13] P.P. Ivanov. *Grounds and Bases of Hydrotechnical Structures.* Visshaya Shkola, Moscow, 1985.

[14] B. Joe. Delaunay Triangular grids in convex polygons. *SIAM J. Sci. Stat. Comput.*, **7**: 514–539, 1986.

[15] K.L. Johnson. *Contact Mechanics*, Cambridge Univ. Press, 1985.

[16] Y.M. Kizyma. Impression of circular punch into elastic layer provided tangential contact tension. *Applied Mechanics*, **9**(8): 112–116, 1973.

[17] K.W. Man. *Contact Mechanics Using Boundary Elements.* Computational Mechanics Publications, Southampton, 1994.

[18] G. Manolis, I. Devies, eds. *Boundary Element Techniques in Geomechanics.* Computational Mechanics Publications, Southampton, 1993.

[19] Z. Olesiak. Annular punch on elastic semi-space. *Arch. Mech. Stos.* **17**: 633–648, 1965.

[20] F.P. Preparata, M.I. Shamos. *Computational Geometry: Introduction.* Springer-Verlag, New York–Berlin, 1985.

[21] V.L. Rvachev, V.S. Procenko. *Contact Problems of the Theory of Elasticity for Non-classical Domains* (in Russian). Naukova Dumka, Kiev, 1977.